Constraints on spin-independent dark matter scattering off electrons with germanium and xenon detectors

Mukesh K. Pandey,[1] Lakhwinder Singh,[2, 3] Chih-Pan Wu,[1] Jiunn-Wei Chen,[4, 5, *]
Hsin-Chang Chi,[6] Chung-Chun Hsieh,[1] C.-P. Liu,[6, †] and Henry T. Wong[2]

[1]*Department of Physics, National Taiwan University, Taipei 10617, Taiwan*
[2]*Institute of Physics, Academia Sinica, Taipei 11529, Taiwan*
[3]*Department of Physics, Banaras Hindu University, Varanasi 221005, India*
[4]*Department of Physics, Center for Theoretical Physics,*
and Leung Center for Cosmology and Particle Astrophysics,
National Taiwan University, Taipei 10617, Taiwan
[5]*Center for Theoretical Physics, Massachusetts Institute of Technology, Cambridge, MA 02139, USA*
[6]*Department of Physics, National Dong Hwa University, Shoufeng, Hualien 97401, Taiwan*
(Dated: January 1, 2019)

Scattering of light dark matter (LDM) particles with atomic electrons is studied in the context of effective field theory. Contact and long-range interactions between dark matter and an electron are both considered. A state-of-the-art many-body method is used to evaluate the spin-independent atomic ionization cross sections of LDM-electron scattering. New upper limits are derived on parameter space spanned by LDM mass and effective coupling strengths using data from the CDMSlite, XENON10, and XENON100 experiments. Comparison with existing calculations shows disagreement and indicates the importance of atomic many-body physics in direct LDM searches.

Introduction. Astronomical and cosmological observations not only provide evidences of dark matter (DM) but also point out its properties such as nonrelativistic, non-baryonic, stable with respect to cosmological time scale, and interacting weakly, if any, with the standard model (SM) particles. Its non-gravitational interactions with normal matter are still unknown. A generic class of cold dark matter candidates, the so-called Weakly-Interacting Massive Particles (WIMPs), receive most attention, as they lead to predictions of DM's relic abundance comparable to the measured value and have coupling strengths of weak interaction scales to SM particles, which can be experimentally tested. Also, the existence of such particles are predicted in many extensions of the SM (see, e.g., Refs. [1, 2] for review). Recently there has been remarkable progress made in direct WIMP searches, thanks to novel innovations in detector technologies and increment of detector size and exposure time. As a result, a substantial portion of the favored WIMP parameter space has now been ruled out. For example, the most stringent bounds on the spin-independent WIMP-nucleon cross section are currently set by the Xenon1T [3]: $4.1 \times 10^{-47} \mathrm{cm}^2$ at $30\,\mathrm{GeV}$ dark matter mass, [1] and PandaX-II [4]: $8.6 \times 10^{-47} \mathrm{cm}^2$ at $50\,\mathrm{GeV}$, respectively.

In spite of tremendous efforts in experiment, no concrete evidence of WIMPs has been found to date, directly or indirectly. This motivates searches of DM particles with masses lighter than generic WIMPs, i.e., $\lesssim 10\,\mathrm{GeV}/c^2$. Theoretically, such light dark matter (LDM) candidates arise in many well-motivated models,

and to account for the relic DM abundance, there are mechanisms suggesting LDM interacts with SM particles through light or heavy mediators with coupling strengths smaller than the weak scale (see Ref. [5] for review). Moreover, annihilations or decays of LDM candidates are possible sources of the anomalous 511 keV [6, 7] and 3.5 keV [8, 9] emission lines recently found in the sky. Consequently, new ideas to search for LDM flourish and have good discovery potential (see Ref. [10] for general survey).

The energy transfer of an incident DM particle to a target particle depends on the reduced mass of the system. Therefore, current direct detection experiments whose energy thresholds for nuclear recoil are a few keV at best can only sensitively search for DM particles with masses as low as a few GeV through DM-nucleus interactions. To go beyond this limit and search for LDM particles, a number of direct detection experiments, such as CRESST-II [11], DAMIC [12], NEWS-G [13], PICO [14], SENSEI [15], and SuperCDMS [16], have intensive research programs pushing towards lower thresholds.

For energy deposition in the sub-keV region, electron recoil becomes an important subject, no matter being taken as a signal or background, because LDM particles transfer their kinetic energy more efficiently to target electrons than nuclei. Furthermore, electron recoil signals can be used to directly constrain LDM-electron interactions; this complements the study of LDM-nucleon interactions through nuclear recoil and extends a direct detector's scientific reach. Constraints of LDM-electron scattering by direct detection experiments emerged recently, e.g., DAMA/LIBRA [17], DarkSide-50 [18], SuperCDMS [19], Xenon10 [20, 21], and Xenon100 [21, 22]; and much improvement will certainly be expected in

---

[1] We use the natural units $\hbar = c = 1$.

next-generation sub-keV detectors.

While electron recoil at sub-keV energies opens a new, exciting window for LDM searches, the scattering processes of LDM particles in detectors pose a fundamental theoretical challenge: The typical energy and momentum of a bound electron is on the order of $Z_{\text{eff}} m_e \alpha$ and $Z_{\text{eff}}^2 m_e \alpha^2/2$, respectively, where Z_{eff} is the effective nuclear charge felt by an electron of mass m_e in a certain shell and α is the fine structure constant with $m_e \alpha \approx 3.7\,\text{keV}$. Consequently a sub-keV scattering event strongly overlaps with the atomic scales. This implies a reliable calculation of LDM-electron scattering cross section, which is needed for data analysis, should properly take into account not only the bound nature of atomic electrons but also the electron-electron correlation.

In this work, we applied a state-of-the-art many-body method to evaluate the atomic ionization cross sections of germanium (Ge) and xenon (Xe) by spin-independent LDM-electron scattering. New upper limits on parameter space spanned by the effective coupling strengths and mass of LDM are derived with data from CDMSlite [23], XENON10 [24] and XENON100 [25]. The results are also compared with existing calculations.

Formalism. A general framework for dark matter interaction with normal matter has recently been developed using effective field theory (EFT). This framework accommodates scalar, fermionic, and vector nonrelativistic (NR) DM particles interacting with NR nucleons via scalar and vector mediators [26]. All leading-order and next-to-leading-order operators in the effective DM-nucleon interaction are identified [27]. The DM-electron interaction can be formulated similarly with the electron being treated relativistically, as it is essential for atomic structure of Ge and Xe [28]. At leading order (LO), the spin-independent (SI) part is parametrized by two terms:

$$\mathcal{L}_{\text{SI}}^{(\text{LO})} = c_1 (\chi^\dagger \chi)(e^\dagger e) + d_1 \frac{1}{q^2} (\chi^\dagger \chi)(e^\dagger e), \qquad (1)$$

where χ and e denote DM and electron fields, respectively, and $q = |\vec{q}|$ is the magnitude of 3-momentum transfer, which can be determined by the NR DM particle's energy transfer T and scattering angle θ. The low-energy constants c_1 and d_1 characterize the strengths of the short-range (for heavy mediators) and long-range (for light mediators) interactions, respectively. While the masses of the mediators can vary in broad ranges, it is customary to consider the two extremes: the extremely massive and the massless, which give rise to the contact (or zero-range) and the (infinitely) long-range interactions, respectively.

The main scattering process that yields electron recoil is atomic ionization:

$$\chi + A \rightarrow \chi + A^+ + e^- , \qquad (2)$$

and the energy deposition by DM is reconstructed by subsequent secondary particles, such as photons and more ionized electrons, recorded in a detector. The differential DM-atom ionization cross section in the laboratory frame through the LO, SI DM-electron interaction is derived in Ref. [28]

$$\frac{d\sigma}{dT} = \frac{m_\chi}{2\pi v_\chi} k_2 \int d\cos\theta \left[\left| c_1 + \frac{d_1}{q^2} \right|^2 \right] R(T,\theta), \qquad (3)$$

where m_χ, v_χ, $k_1 = m_\chi v_\chi$ and $k_2 = (m_\chi^2 v_\chi^2 - 2m_\chi T)^{1/2}$ are the mass, velocity, initial and final momentum of the DM particle, respectively.

The full information of how the detector atom responds to the incident DM particle is encoded in the response function

$$R(T,\theta) = 4\pi \sum_{i=1}^{Z} \int d^3 p_i \, | \langle A^+, e^- || e^{i \frac{\mu}{m_e} \vec{q} \cdot \vec{r}_i} || A \rangle |^2$$
$$\times \delta(T - E_{B_i} - \frac{\vec{q}^2}{2M} - \frac{\vec{p_i}^2}{2\mu}), \qquad (4)$$

where $|A\rangle$ and $|A^+, e^-\rangle$ denote the many-body initial (bound) and final (ionized) state; M and μ the total and reduced mass of the ion plus free electron system, respectively, with $\mu \approx m_e$. The summation is over all electrons, and the ith electron has its binding energy E_{B_i}, relative coordinate $\vec{r}_i$, and relative momentum $\vec{p}_i$. The Dirac delta function imposes energy conservation and constrains the kinematics of the ejected electron, whose energy is NR in the kinematic range of our study but wave function still in the fully relativistic form.

Evaluation of $R(T,\theta)$ is non-trivial. In this work, we use a well-benchmarked procedure based on an *ab inito* method, the (multi-configuration) relativistic random phase approximation, (MC)RRPA [29–33]. Details of how the theory was applied to the responses of Ge and Xe detectors in cases of neutrino scattering are documented in Refs. [34–37]; here we only give a brief outline and focus on the points that are new in the case of LDM scattering.

First, the ground-state atomic wave functions are calculated by (MC) Dirac-Fock (DF) theory. The multi-configuration feature is needed for open-shell atoms like Ge, but not for noble gas atoms like Xe. Quality of the initial wave function is benchmarked by the ionization energies of all atomic shells, which can be determined by edges in photoabsorption data.

Second, (MC)RRPA is applied to calculate the transition matrix elements of photoionization. Quality of the final state wave function is benchmarked by how good the calculated photoionization cross section is compared with experiment data. For Ge and Xe, the atomic numbers $Z = 32$ and 54 are not small, so relativistic corrections to inner-shell electrons, which contribute most to the cross section when energy transfer is in the sub-keV to keV range, are sizable. Furthermore, the residual

electron correlation is important for excited states, as a result, its (partial) inclusion by RPA makes our calculated photoionization cross sections of Ge and Xe in excellent agreement with experiments. The only exception is $T < 80$ eV for Ge, where the crystal structure of outer-shell electrons in Ge semiconductor can not be described by our pure atomic calculations [34, 36].

Taking the well-benchmarked initial and final state wave functions, response functions for DM-atom scattering, Eq. (4), are computed, in a similar procedure as we previously did for neutrino-atom scattering. To expedite the computation, we performed (MC)RRPA calculations only for selected data points, and the full computation is done with an additional approximation: the frozen-core approximation (FCA). In this scheme, the final-state continuum wave function of the ionized electron is solved by the Dirac equation which has an electromagnetic mean field determined from the ionic state given by (MC)DF. Compared with the (MC)RRPA, the FCA has a discrepancy less than 20% for all the results reported in the work.

At a direct detector, the measured event rate is

$$\frac{d\mathcal{R}}{dT} = \frac{\rho_\chi \, N_T}{m_\chi} \frac{d\langle\sigma v_\chi\rangle}{dT}, \tag{5}$$

where $\rho_\chi = 0.4$ GeV/cm^3 is the local DM density [38], and N_T is the number of target atoms. The averaged velocity-weighted differential cross section

$$\frac{d\langle\sigma v_\chi\rangle}{dT} = \int_{v_{\min}}^{v_{\mathrm{esc}}} d^3 v_\chi f(\vec{v}_\chi) v_\chi \frac{d\sigma}{dT}, \tag{6}$$

is folded to the conventional Maxwell-Boltzmann velocity distribution $f(\vec{v}_\chi)$ with parameters taken from Ref. [39], the galactic escape velocity $v_{\mathrm{esc}} = 544$ km/s [40], and $v_{\min} = \sqrt{2T/m_\chi}$ to guarantee enough kinetic energy.

In Fig. 1, we show some results of $d\langle\sigma v_\chi\rangle/dT$ for Ge and Xe targets with selected LDM masses. There are several noticeable features. First, the sharp edges correspond to ionization thresholds of specific atomic shells. They clearly indicate the effect of atomic structure, and the peak values sensitively depend on atomic calculations. If direct DM detectors have good enough energy resolution, these peaks can serve as powerful statistical hot spots. Second, away from these edges, the comparison between Ge and Xe cases do point out that the latter has a larger cross section, but the enhancement is not as strong as Z^2 for coherent scattering nor Z for incoherent sum of free electrons. In other words, a heavier target atom does not enjoy much advantage in constraining the SI DM-electron interaction, in opposition to the SI DM-nucleon case. Third, the long-range interaction has a larger inverse energy dependence than the short-range one. As a result, lowering threshold can effectively boost a detector's sensitivity to the long-range DM-electron interaction.

Results and Discussions The CDMSlite experiment with Ge-crystals as target has recently demonstrated the novel mechanism of bolometric amplification [41] and achieved low ionization threshold making it sensitive to LDM searches. A data set of 70.1 kg-day exposure [23] and threshold of 80 eV is adopted for this analysis. The combined trigger and pulse-shape analysis efficiency is more than 80%. Limits on LDM-electron scattering are derived without background subtraction with optimum interval method [42]. The derived 90% C.L. limits for both short- and long-range coupling are depicted in Fig. 2.

Dual-phase liquid Xe detectors have demonstrated the sensitivity to ionization of a single electron with their "S2-only" signals [43]. Constraints have been placed in Refs. [20, 21] with XENON10 [24] and XENON100 [25] data on LDM-electron scattering using an alternative theoretical framework with different treatment to the atomic physics from this work.

Efficiency-corrected data of XENON10 [20, 24] with 15 kg-day exposure and XENON100 [25] with 30 kg-year exposure are extracted from the literature. We follow the same procedure of Refs. [20, 21] to convert energy transfer T first to the number of secondary electrons, n_e, and then to the photoelectron (PE) yield. Under a conservative assumption that all observed events are from potential LDM-electron scattering, upper limits at 90% C.L. on both short- and long-range interactions are derived and displayed in Fig. 2.

Comparing the various exclusion curves in Fig. 2, there are several important observations to note. First, the lowest reach of a direct search experiment in LDM mass is determined by its energy threshold. According to what we set for CDMSlite, XENON100, and XENON10: 80, 56, and 13.8 eV, the lightest DM masses can be probed are $\sim$ 50, 30, and 10 MeV, respectively. The exclusion limits on DM-electron interaction strengths depend on several factors: Experimentally, detector species, energy resolution, background, and exposure mass-time all come into play [44]. Theoretically, the DM-electron interaction type and the atomic structure do matter. For the contact interaction, where the DM-Xe differential cross section is universally bigger than the DM-Ge one, XENON100 gives a better limit than CDMSlite is mainly due to its larger exposure mass-time. On the other hand, the very low threshold of XENON10 not only makes it able to constrain the lower-mass region where XENON100 has no observable electron recoil signals (evidenced by the turning point at $m_\chi \sim 50$ MeV in the left panel of Fig. 2), but also results in a slightly better limit than XENON100, despite a smaller exposure mass-time by almost three orders of magnitude. The exclusion limit on the long-range interaction is also subtle. As pointed out earlier that its differential cross section has a sharper energy dependence and weights more at low T, this explains why XENON10's constraint is much better than oth-
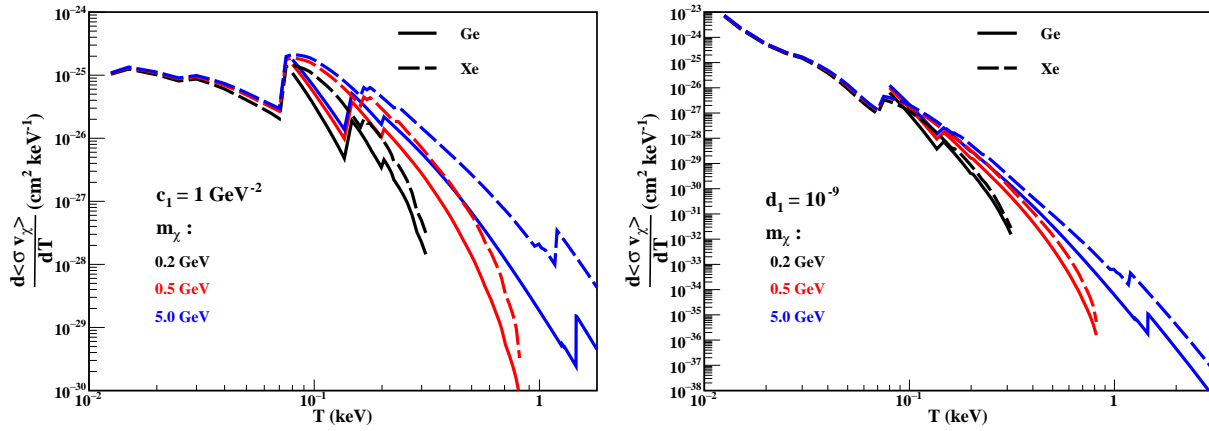
FIG. 1. Averaged velocity-weighted differential cross sections for ionization of Ge and Xe atoms by LDM of various masses with the effective short-range (left) and long-range (right) interactions where $c_1 = 1/\text{GeV}^{-2}$ and $d_1 = 10^{-9}$.

ers in the entire plot. Also for the low-energy weighting, the finer energy resolution and lower background of CDMSlite makes its power to constrain d_1 better than XENON100.

In Fig. 2, the exclusion limits derived in Ref. [21], using the same XENON10 and XENON100 data, are compared. [2] The differences in the overall exclusion curves are obvious and most likely of theoretical origins. In Fig. 3, we use a sample case to illustrate the difference in predicted event numbers as a function of n_e. For both types of interactions, our results are comparatively smaller at small n_e but bigger at large n_e. This provides a qualitative explanation for the overall differences observed in the exclusion curves: The larger the DM mass m_χ, the larger its kinetic energy and hence the increasing chance of higher energy scattering that produces more n_e. Therefore, our calculations yield tighter constraints on c_1 for heavier DM particles, but looser for lighter DM particles. As for the long-range interaction, the low-energy cross section is so dominant that the derivation of exclusion limit is dictated by the one-electron event, i.e., the first bin. As a result, the larger event number (by about one order of magnitude) predicted in Ref. [21] leads to a better constraint on d_1 by a similar size.

The theoretical discrepancy shown in Fig. 3 is certainly puzzling. State-of-the-arts atomic calculations such as (MC)RRPA are typically good at the level of a few percent, but even with a very conservative 20% error we estimate for our frozen core approximation, it is not enough to accommodate the difference. We emphasize that the success of (MC)RRPA in benchmarking the initial and final many-body wave functions of Ge and Xe critically depend on its being a relativistic treatment and inclusion

of electron-electron correlation, which is known to be important particularly for excited states. Compared with the nonrelativistic and purely mean-field treatments of Refs. [18, 20, 21, 45], our approach should be considered a better starting point to calculate the atomic ionization by LDM. Meanwhile, given the important implication of these calculations, the theoretical discrepancy we report in this paper should be known to the communities and further investigation of related atomic many-body problems warranted.

---

* jwc@phys.ntu.edu.tw; corresponding author
† cpliu@mail.ndhu.edu.tw; corresponding author

[1] M. Tanabashi *et al.* (Particle Data Group), Phys. Rev. D **98**, 030001 (2018).

[2] G. Arcadi, M. Dutra, P. Ghosh, M. Lindner, Y. Mambrini, M. Pierre, S. Profumo, and F. S. Queiroz, Eur. Phys. J. C **78**, 203 (2018), arXiv:1703.07364 [hep-ph].

[3] E. Aprile *et al.* (XENON Collaboration), Phys. Rev. Lett. **121**, 111302 (2018).

[4] X. Cui *et al.* (PandaX-II), Phys. Rev. Lett. **119**, 181302 (2017).

[5] R. Essig *et al.*, in *Proceedings, 2013 Community Summer Study on the Future of U.S. Particle Physics: Snowmass on the Mississippi (CSS2013): Minneapolis, MN, USA, July 29-August 6, 2013* (2013) arXiv:1311.0029 [hep-ph].

[6] J. Knodlseder *et al.*, Astron. Astrophys. **441**, 513 (2005), arXiv:astro-ph/0506026 [astro-ph].

[7] D. P. Finkbeiner and N. Weiner, Phys. Rev. D **76**, 083519 (2007), arXiv:astro-ph/0702587 [astro-ph].

---

[2] The conversion $\sigma_e = c_1^2 \mu_{\chi e}^2/\pi$ and $\bar{\sigma}_e = d_1^2 \mu_{\chi e}^2 / \left(\pi(m_e \alpha)^4\right)$ with $\mu_{\chi e} = m_\chi m_e/(m_\chi + m_e)$ is used.
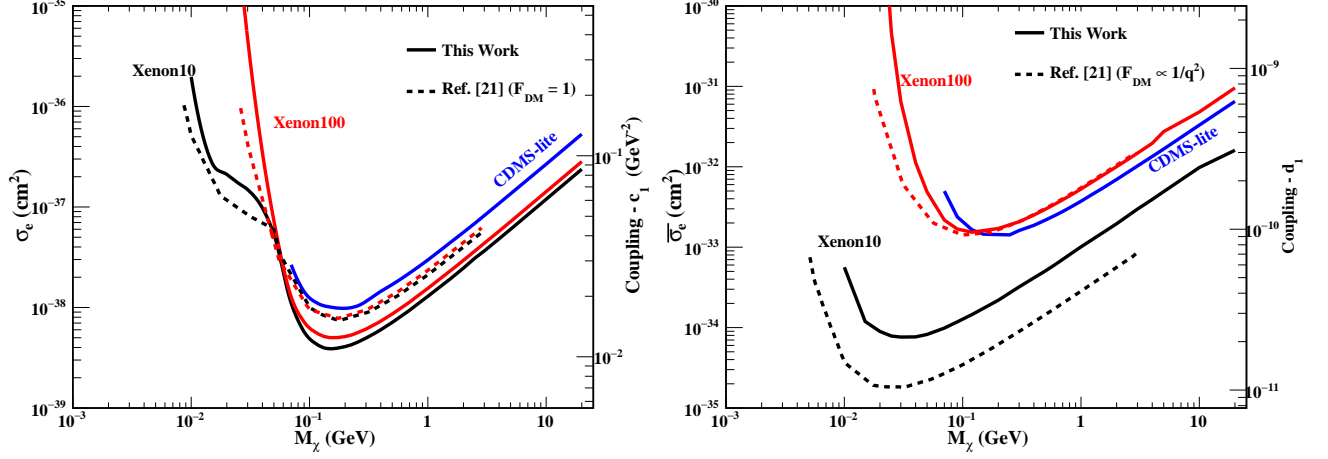
FIG. 2. Exclusion limits at 90% C.L. on the spin-independent short-(left) and long-(right) range LDM-electron interactions as functions of m_χ derived from CDMSlite (blue) [23], Xenon100 (red) [25], and Xenon10 (black) [24] data. Superimposed are constraints from Ref. [21] using XENON10 (black-dotted) and XENON100 (red-dotted), in which the choices of $F_{DM} = 1$ (left) and $F_{DM} = 1/q^2$ (right) correspond to c_1- and d_1-type interactions, respectively, in this work.
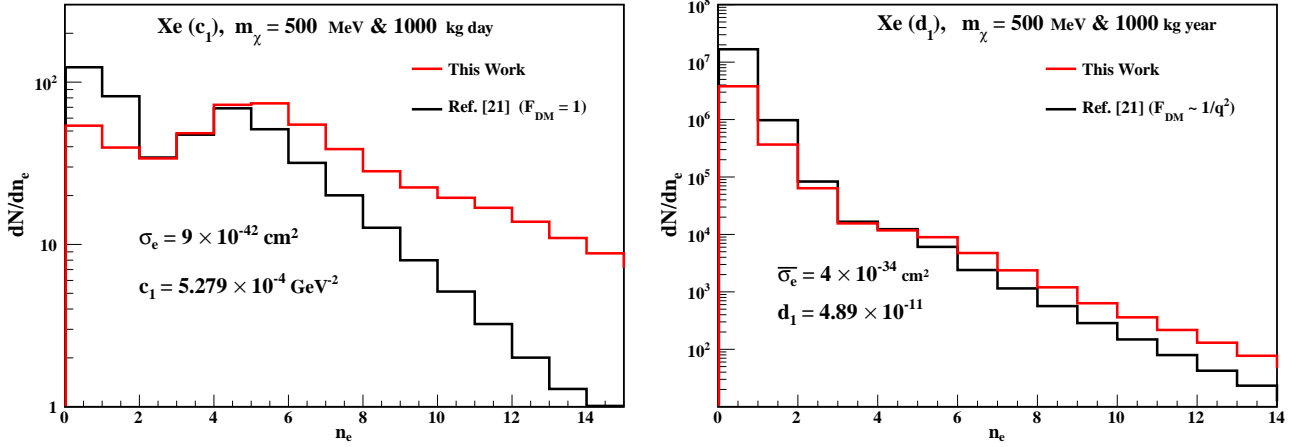

FIG. 3. Comparisons of expected event numbers as a function of ionized electron number derived in this work (red lines) and from Ref. [21] (black lines) for Xe detectors with 1000 kg-year exposure, assuming DM mass $m_\chi = 500\,\mathrm{MeV}$, and DM-electron interaction strengths (left) $c_1 = 5.28 \times 10^{-4}\,\mathrm{GeV}^{-2}$ and (right) $d_1 = 4.89 \times 10^{-11}$ (equivalent to $\sigma_e = 9 \times 10^{-42}\,\mathrm{cm}^2$ and $\bar{\sigma}_e = 4 \times 10^{-34}\,\mathrm{cm}^2$, respectively in Ref. [21]).

[8] E. Bulbul, M. Markevitch, A. Foster, R. K. Smith, M. Loewenstein, *et al.*, Astrophys. J. **789**, 13 (2014), arXiv:1402.2301 [astro-ph.CO].

[9] A. Boyarsky, O. Ruchayskiy, D. Iakubovskyi, and J. Franse, Phys. Rev. Lett. **113**, 251301 (2014), arXiv:1402.4119 [astro-ph.CO].

[10] M. Battaglieri *et al.*, in *U.S. Cosmic Visions: New Ideas in Dark Matter College Park, MD, USA, March 23-25, 2017* (2017) arXiv:1707.04591 [hep-ph].

[11] G. Angloher *et al.* (CRESST), Eur. Phys. J. C **76**, 25 (2016), arXiv:1509.01515 [astro-ph.CO].

[12] J. Barreto *et al.* (DAMIC), Phys. Lett. B **711**, 264 (2012).

[13] Q. Arnaud *et al.* (NEWS-G), Astropart. Phys. **97**, 54 (2018), arXiv:1706.04934 [astro-ph.IM].

[14] C. Amole *et al.* (PICO Collaboration), Phys. Rev. Lett. **118**, 251301 (2017).

[15] J. Tiffenberg *et al.* (SENSEI), Phys. Rev. Lett. **119**, 131802 (2017), arXiv:1706.00028 [physics.ins-det].

[16] R. Agnese *et al.* (SuperCDMS), Phys. Rev. Lett. **116**, 071301 (2016), arXiv:1509.02448 [astro-ph.CO].

[17] B. M. Roberts *et al.*, Phys. Rev. D **93**, 115037 (2016).

[18] P. Agnes *et al.* (The DarkSide Collaboration), Phys. Rev. Lett. **121**, 111303 (2018).

[19] R. Agnese *et al.* (SuperCDMS), Phys. Rev. Lett. **121**, 051301 (2018), arXiv:1804.10697 [hep-ex].

[20] R. Essig *et al.*, Phys. Rev. Lett. **109**, 021301 (2012).

[21] R. Essig, T. Volansky, and T.-T. Yu, Phys. Rev. D **96**, 043017 (2017), arXiv:1703.00910 [hep-ph].

[22] E. Aprile *et al.* (XENON100), Science **349**, 851 (2015).

[23] R. Agnese *et al.* (SuperCDMS), Phys. Rev. D **97**, 022002 (2018), arXiv:1707.01632 [astro-ph.CO].

[24] J. Angle *et al.* (XENON10), Phys. Rev. Lett. **107**, 051301 (2011), [Erratum: Phys. Rev. Lett.110,249901(2013)],

arXiv:1104.3088 [astro-ph.CO].

[25] E. Aprile *et al.* (XENON100), Phys. Rev. D **94**, 092001 (2016), [Erratum: Phys. Rev. D95, no.5, 059901(2017)], arXiv:1605.06262 [astro-ph.CO].

[26] J. Fan, M. Reece, and L.-T. Wang, JCAP **1011**, 042 (2010), arXiv:1008.1591 [hep-ph].

[27] A. L. Fitzpatrick *et al.*, JCAP **1302**, 004 (2013).

[28] J.-W. Chen, H.-C. Chi, C.-P. Liu, C.-L. Wu, and C.-P. Wu, Phys. Rev. D **92**, 096013 (2015), arXiv:1508.03508 [hep-ph].

[29] W. R. Johnson and C. D. Lin, Phys. Rev. A **20**, 964 (1979).

[30] W. R. Johnson and K. T. Cheng, Phys. Rev. A **20**, 978 (1979).

[31] K.-N. Huang and W. R. Johnson, Phys. Rev. A **25**, 634 (1982).

[32] K.-N. Huang, Phys. Rev. A **26**, 734 (1982).

[33] K.-N. Huang, H.-C. Chi, and H.-S. Chou, Chin. J. Phys. **33**, 565 (1995).

[34] J.-W. Chen, H.-C. Chi, K.-N. Huang, C.-P. Liu, H.-T. Shiao, L. Singh, H. T. Wong, C.-L. Wu, and C.-P. Wu, Phys. Lett. B **731**, 159 (2014), arXiv:1311.5294 [hep-ph].

[35] J.-W. Chen, H.-C. Chi, H.-B. Li, C. P. Liu, L. Singh, H. T. Wong, C.-L. Wu, and C.-P. Wu, Phys. Rev. D **90**, 011301 (2014), arXiv:1405.7168 [hep-ph].

[36] J.-W. Chen, H.-C. Chi, K.-N. Huang, H.-B. Li, C.-P. Liu, L. Singh, H. T. Wong, C.-L. Wu, and C.-P. Wu, Phys. Rev. D **91**, 013005 (2015), arXiv:1411.0574 [hep-ph].

[37] J.-W. Chen, H.-C. Chi, C. P. Liu, and C.-P. Wu, Phys. Lett. B **774**, 656 (2017), arXiv:1610.04177 [hep-ex].

[38] R. Catena and P. Ullio, JCAP **1008**, 004 (2010).

[39] J. Lewin and P. Smith, Astropart.Phys. **6**, 87 (1996).

[40] M. C. Smith *et al.*, Mon. Not. Roy. Astron. Soc. **379**, 755 (2007), arXiv:astro-ph/0611671 [astro-ph].

[41] R. Agnese *et al.* (SuperCDMS), Phys. Rev. Lett. **112**, 041302 (2014), arXiv:1309.3259 [physics.ins-det].

[42] S. Yellin, (2008), arXiv:0709.2701 [physics.data-an].

[43] E. Aprile *et al.* (XENON), Astropart. Phys. **34**, 679 (2011), arXiv:1001.2834 [astro-ph.IM].

[44] T. Marrodán Undagoitia and L. Rauch, J. Phys. G **43**, 013001 (2016), arXiv:1509.08767 [physics.ins-det].

[45] R. Essig, J. Mardon, and T. Volansky, Phys. Rev. D **85**, 076007 (2012), arXiv:1108.5383 [hep-ph].